J|A|C|S
ARTICLES

Published on Web 09/26/2008

Probing the Self-Assembly of Inorganic Cluster Architectures in Solution with Cryospray Mass Spectrometry: Growth of Polyoxomolybdate Clusters and Polymers Mediated by Silver(I) Ions

Elizabeth F. Wilson,[†] Hamera Abbas,[†] Bridgette J. Duncombe,[‡] Carsten Streb,[†] De-Liang Long,[†] and Leroy Cronin*,[†]

Department of Chemistry, WestCHEM, The University of Glasgow, University Avenue, Glasgow, G12 8QQ, U.K., and Department of Chemistry, and EastCHEM, The University of Edinburgh, West Mains Road, Edinburgh, EH9 3JJ, U.K.

Received April 6, 2008; E-mail: L.Cronin@chem.gla.ac.uk

Abstract: Cryospray mass spectrometry (CSI-MS) has been used to probe the mechanism of self-assembly of polyoxometalate clusters in solution. By using CSI-MS and electronic absorbance spectroscopy it was possible to monitor in real-time the self-assembly of polymeric chains based on $[Ag_2Mo_8O_{26}]^{2-}{}_n$ building blocks. The role of the Ag^I ion in the solution state rearrangement of molybdenum Lindqvist ({Mo_6}) into the silver-linked β-octamolybdate ({Mo_8}) structure $((n\text{-}C_4H_9)_4N)_{2n}[Ag_2Mo_8O_{26}]_n$ (**1**) is revealed in unprecedented detail. A monoanionic series, in particular $[AgMo_mO_{3m+1}]^-$ where $m = 2$ to 4, and series involving mixed oxidation state polyoxomolybdate species, which illustrate the in-solution formation of the (Ag{Mo_8}Ag) building blocks, have been observed. CSI-MS detection of species with increasing metal nuclearity concomitant with increasing organic cation contribution supports the hypothesis that the organic cations used in the synthesis play an important structure-directing role in polyoxometalate (POM) growth in solution. A real-time decrease in [{Mo_6}] and associated increase in [{Mo_8}] have been observed using CSI-MS and electronic absorbance spectroscopy, and the rate of {Mo_6} interconversion to {Mo_8} was found to decrease on increasing the size of the countercation. This result can be attributed to the steric bulk of larger organic groups hindering {Mo_6} to {Mo_8} rearrangement and hindering the contact between silver cations and molybdenum anions.

Introduction

Polyoxometalate (POM) clusters constitute a wide and varied family of structures formed *via* condensation reactions of metal oxide anions of early transition metals in high oxidation states, e.g., V, Mo, W.[1,2] The capacity of these clusters to bridge multiple length scales, from subnanoscale to protein sized molecules,[3,4] coupled with their attractive electronic and molecular properties,[5] gives rise to a wide variety of applications of these structures, e.g., in catalysis,[5,6] medicine,[1,2] and materials science.[7−9]

One of the most interesting aspects of POM chemistry lies with the fact that the clusters can be viewed as transferable building blocks or synthons.[10] As such the controlled assembly of polyoxometalate-based building blocks defines a crucial challenge to engineer these building fragments so they can assemble into novel architectures with functionality. However, despite the increasingly intensive research in this area, understanding of the complex formation mechanisms and self-assembly processes which govern POM structure formation remains limited.[10−12] In practice, this lack of understanding leads to experimentation where manipulation of reaction parameters in the commonly used "one-pot" POM syntheses often leads to the formation of new POM structures, all be it *via* a somewhat serendipitous approach.[3,4] Although the fundamental speciation process underlying the formation of low nuclearity molybdates and tungstates is well understood,[4] the process by which larger or polymeric structures are formed is not clear due to the vast

[†] The University of Glasgow.
[‡] The University of Edinburgh.

(1) Gouzerh, P.; Proust, A. *Chem. Rev.* **1998**, *98*, 77–111.
(2) Rhule, J. T.; Hill, C. L.; Judd, D. A. *Chem. Rev.* **1998**, *98*, 327–357.
(3) Müller, A.; Beckmann, E.; Bogge, H.; Schmidtmann, M.; Dress, A. *Angew. Chem., Int. Ed.* **2002**, *41*, 1162–1167.
(4) Cronin, L. High Nuclearity Polyoxometalate Clusters. In *Comprehensive Coordination Chemistry II*; McLeverty, J. A., Meyer, T. J., Eds.; Elsevier Publishers: Amsterdam, The Netherlands, 2004; Vol.7, pp 1−57.
(5) (a) Katsoulis, D. E. *Chem. Rev.* **1998**, *98*, 359–387. (b) Yamase, T. *Chem. Rev.* **1998**, *98*, 307–325. (c) Kozhevnikov, I. V. *Chem. Rev.* **1998**, *98*, 171–198.
(6) Rhule, J. T.; Neiwert, W. A.; Hardcastle, K. I.; Do, B. T.; Hill, C. L. *J. Am. Chem. Soc.* **2001**, *123*, 12101–12102.
(7) Zeng, H. D.; Newkome, G. R.; Hill, C. L. *Angew. Chem., Int. Ed.* **2000**, *39*, 1772–1774.
(8) Ogliaro, F.; de Visser, S. P.; Cohen, S.; Sharma, P. K.; Shaik, S. *J. Am. Chem. Soc.* **2002**, *124*, 2806–2817.
(9) Streb, C.; Ritchie, C.; Long, D. -L.; Kögerler, P.; Cronin, L. *Angew. Chem., Int. Ed.* **2007**, *46*, 7579–7582.
(10) Long, D.-L.; Burkholder, E.; Cronin, L. *Chem. Soc. Rev.* **2007**, *36*, 105–121.
(11) Müller, A.; Peters, F.; Pope, M. T.; Gatteschi, D. *Chem. Rev.* **1998**, *98*, 239–271.
(12) Xu, L.; Lu, M.; Xu, B.; Wei, Y.; Peng, Z.; Powell, D. R. *Angew. Chem., Int. Ed.* **2002**, *41*, 4129–4131.

10.1021/ja802514q CCC: $40.75

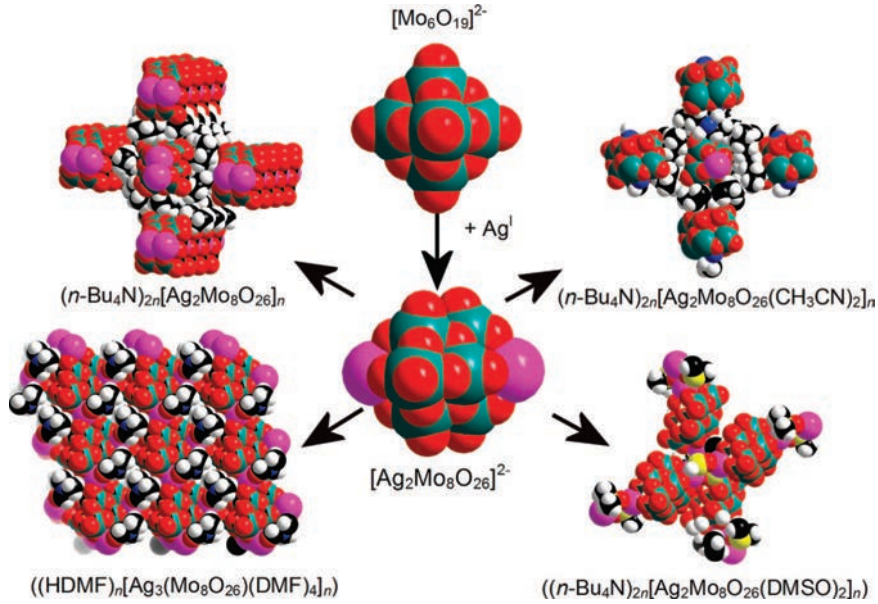

Figure 1. Scheme showing the transformation of the Lindqvist anion, $[Mo_6O_{19}]^{2-}$, into the $[Ag_2Mo_8O_{26}]^{2-}$ building block (center) which subsequently forms a variety of POM cluster architectures in the solid state.[17,18] Color scheme: Mo, green; Ag, pink; O, red; C, black; H, white; S, yellow.

combinatorial library of cluster types/repeat units potentially available as the number of building blocks increase.[10] Thus, there is a clear need to develop approaches to bridge the gap[13] between solid state and solution studies so that the key features of the mechanism of the self-assembly of polyoxometalate clusters can be unveiled.

To stabilize particular POM building blocks in solution, and so allow mechanistic insight into the formation of different POM architectures, we have developed an approach to POM synthesis which uses bulky organic cations to "direct" the structure growth.[14−16] This has been illustrated in previous work by us in which the use of protonated hexamethylenetetramine ($HMTAH^+$) as counterions enabled stabilization and isolation of the highly charged polyoxomolybdate anion, $[H_2Mo^V_4Mo^{VI}_{16}O_{52}]^{10-}$,[14,15] followed by the isolation of a family of sulfite-based Dawson-type mixed-valence polyoxomolybdates $[Mo_{18}O_{54}(SO_3)_2]^{n-}$, using the same synthetic approach.[16] In particular, this "encapsulating" organic cation method was utilized to investigate different chain length alkylammonium salts of the well-known molybdenum Lindqvist, $[Mo_6O_{19}]^{2-}$, anion ($\{Mo_6\}$) in reactions with electrophilic silver(I) ions; see Figure 1.[17,18] This work produced a family of Ag-substituted, polymeric POM architectures consisting of β-octamolybdate, β-$[Mo^{VI}_8O_{26}]^{4N}$, ($\{Mo_8\}$) building blocks linked through coordination to electrophilic silver(I) ions.[17−19] It was this rearrangement of the Lindqvist anion into the silver-linked octamolybdate synthons making up the structures of this family of POM architectures which ignited our interest to study the formation of this particular reaction system further.

Therefore, given the enormous challenge presented to follow the self-assembly process we set out to use cryospray mass spectrometry (CSI-MS), with a high resolution time-of-flight detector (TOF), and electronic absorbance spectroscopy, to investigate the self-assembly of polyoxometalate clusters in solution. We have been developing the application of CSI-MS with a high resolution TOF detector to study labile POM systems.[20] This is because ESI-MS studies of such systems have been limited by the use of low resolution detectors and the high desolvation temperatures utilized in the ESI process,[21] the majority of ionic species observed when studying labile POM structures with this ionization source still being highly ionized, multiply charged species.[22−24] This is indicative that fragmentation of labile POM clusters occurs at the relatively high temperatures (150−200 °C) used to desolvate during the ESI process. In contrast, the low temperatures accessible (minimum −100 °C) for use with a cryospray source minimize uncontrolled fragmentation and so allow efficient transfer of very high nuclearity, yet labile, ionic species into the detector with minimal interfering effects from the ionization and desolvation processes.[25] By employing this approach it is then possible to transmit many of the labile species present in solution into the mass spectrometer and so allow some correlation between the essentially gas phase measurements with solution and solid state studies.[20,25]

(13) Cooper, G. J. T.; Newton, G. N.; Kögerler, P.; Long, D.-L.; Engelhardt, L.; Luban, M.; Cronin, L. *Angew. Chem., Int. Ed.* **2007**, *46*, 1340–1344.
(14) Long, D.-L.; Kögerler, P.; Farrugia, L. J.; Cronin, L. *Angew. Chem., Int. Ed.* **2003**, *42*, 4180–4183.
(15) Long, D.-L.; Abbas, H.; Kögerler, P.; Cronin, L. *J. Am. Chem. Soc.* **2004**, *126*, 13880–13881.
(16) Long, D.-L.; Kögerler, P.; Cronin, L. *Angew. Chem., Int. Ed.* **2004**, *43*, 1817–1820.
(17) Abbas, H.; Pickering, A. L.; Long, D. -L.; Kögerler, P.; Cronin, L. *Chem.—Eur. J.* **2005**, *11*, 1071–1078.
(18) Abbas, H.; Streb, C.; Pickering, A. L.; Neil, A. R.; Long, D.-L.; Cronin, L. *Cryst. Growth Des.* **2008**, *8*, 635–642.
(19) Chen, S. M.; Lu, C. Z.; Yu, Y. Q.; Zhang, Q. Z.; He, X. *Inorg. Chem. Commun.* **2004**, *7*, 1041–1044.
(20) Miras, H. N.; Long, D.-L.; Kögerler, P.; Cronin, L. *J. Chem. Soc., Dalton Trans.* **2008**, 214–221.
(21) Long, D.-L.; Streb, C.; Song, Y. F.; Mitchell, S.; Cronin, L. *J. Am. Chem. Soc.* **2008**, *130*, 1830–1832.
(22) Bonchio, M.; Bortolini, O.; Conte, V.; Sartorel, A. *Eur. J. Inorg. Chem.* **2003**, *4*, 699–704.
(23) Walanda, D. K.; Burns, R. C.; Lawrance, G. A.; von Nagy-Felsobuki, E. I. *J. Chem. Soc., Dalton Trans.* **1999**, *3*, 311–321.
(24) Walanda, D. K.; Burns, R. C.; Lawrance, G. A.; von Nagy-Felsobuki, E. I. *J. Cluster Sci.* **2000**, *11*, 5–28.
(25) Deery, M. J.; Howarth, O. W.; Jennings, K. R. *J. Chem. Soc., Dalton Trans.* **1997**, 4783–4788.

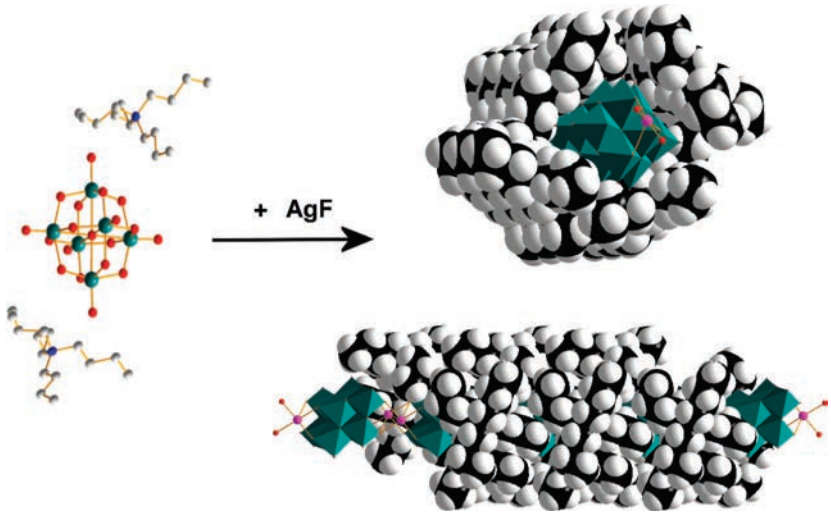

Figure 2. A schematic showing the formation of the polymeric POM architecture $TBA_{2n}[Ag_2Mo_8O_{26}]_n$ (**1**) on the reaction of $TBA_2[Mo_6O_{19}]$ with AgF. Left: $TBA_2[Mo_6O_{19}]$ unit is shown in ball and stick representation. Color scheme: Mo, green; O, red; C, light gray; N, blue. Right: Two structural representations of **1** are shown with the silver-linked β-octamolybdate chain (ball and stick, and green polyhedra) wrapped in the "encapsulating" TBA^+ cations (space-filling representation). A side view along the $\{Ag_2Mo_8\}_\infty$ chain (bottom right) and end-on view of this chain (top right) are shown. Color scheme: Mo, green polyhedra; Ag, pink; O, red; C, black; H, white.

However, it is also possible that when using the technique of CSI-MS, the CSI-MS determined concentration of sensitive species (i.e., sensitive to changes in pH or the presence of other species) can still differ to some extent from that determined in bulk measurements. This effect was investigated by Howarth et al. during ESI-MS studies[25] and is due to the interference in the equilibrium process by the drying agent (e.g., nitrogen gas) as the desolvation rapidly affects the pH and the concentrations of the solutes in the formation of the analytes.

For this work, the use of CSI-MS in conjunction with electronic absorbance spectroscopy was selected, not only to identify species present in the reaction mixture of the chosen POM reaction system but also to allow real-time monitoring of the Lindqvist rearrangement into the silver-linked octamolybdate species. The combined application of these analytical techniques to monitor real-time, in-solution rearrangements in a POM reactant solution is unprecedented, with previous studies focusing on the isolated use of electronic absorbance spectroscopic data[26] or electron spin resonance[27] to study the formation of heteropolyoxomolybdates. This approach opens the door to further exploration and expansion of our understanding of the building block principles which govern the bottom-up processes in solution and will lead us to future methods for control of these building processes.

In this current work the in-solution interconversion of Lindqvist into β-octamolybdate anions and subsequent self-assembly into the silver-linked POM structure $((n\text{-}C_4H_9)_4N)_{2n}[Ag_2Mo_8O_{26}]_n$ (**1**)[17] has been investigated using CSI-MS and electronic absorbance spectroscopy. These techniques have been utilized in this study to probe the rearrangements occurring in the reaction solution from which compound **1** crystallizes, the kinetics of these self-assembly processes, and the effect of organic cation size on the kinetics of these processes.

Results and Discussion

The rearrangement of the molybdenum Lindqvist to form the β-octamolybdate anion has previously only been observed indirectly *via* the crystallization of silver-linked β-octamolybdate species such as compound **1**,[17,19] $((n\text{-}C_4H_9)_4N)_{2n}[Ag_2Mo_8O_{26}]_n$ (also referred to as $TBA_{2n}[Ag_2Mo_8O_{26}]_n$).

This compound is produced by the reaction of $((n\text{-}C_4H_9)_4N)_2[Mo_6O_{19}]$ (also referred to as $TBA_2[Mo_6O_{19}]$) with silver(I) fluoride in a methanol and acetonitrile mixture. The flexible tetrabutylammonium cations (TBA^+) wrap around and encapsulate the linear chain of linked $[Ag^IMo^{VI}{}_8O_{26}Ag^I]^{2-}$ units; see Figure 2. X-ray crystallographic studies of the solid state of **1** have shown that these encapsulating cations are packed into a network of collinear, organic "tunnels" along which the polymeric chains of $\{Ag_2Mo_8\}_n$ anions propagate.[17] The silver(I) centers of these anions form virtually planar O_2AgO_2 bridging groups which result in close Ag−Ag contacts (2.8531(4)Å) that are shorter than metallic Ag···Ag distances, suggesting significant argentophilic silver(I)−silver(I) interactions.[28]

Through this work[17] the nature of the $\{Ag_2\}$ linker groups and the Ag coordination environments were found to be strongly dependent on the reaction conditions, and it can be suggested that the precursors in the reaction solution were not individual $\{Ag_2\}$ and $\{Mo_8\}$ groups but, most likely, the $(Ag\{Mo_8\}Ag)$-type building blocks; see Figure 3. Furthermore, the mode of assembly of these synthon units in the solid state is critically dependent on the reaction conditions. This is illustrated by the use of different chain length organic cations and solvent systems which demonstrated a strategy to control the molecular growth processes from $(Ag\{Mo_8\}Ag)^{2-}$ building blocks to linear molecular chains and grids.[18]

Here we report the first direct observation of the self-assembly aggregation and rearrangement processes which govern POM formation in solution. This investigation was carried out using

(26) Nolan, A. L.; Burns, R. C.; Lawrance, G. A.; Craig, D. C. *J. Chem. Soc., Dalton Trans.* **1996**, 2629–2636.
(27) Angus-Dunne, S. J.; Irwin, J. A.; Burns, R. C.; Lawrance, G. A.; Craig, D. C. *J. Chem. Soc., Dalton Trans.* **1993**, 2717–2726.
(28) Jansen, M. *Angew. Chem., Int. Ed.* **1987**, *26*, 1098.

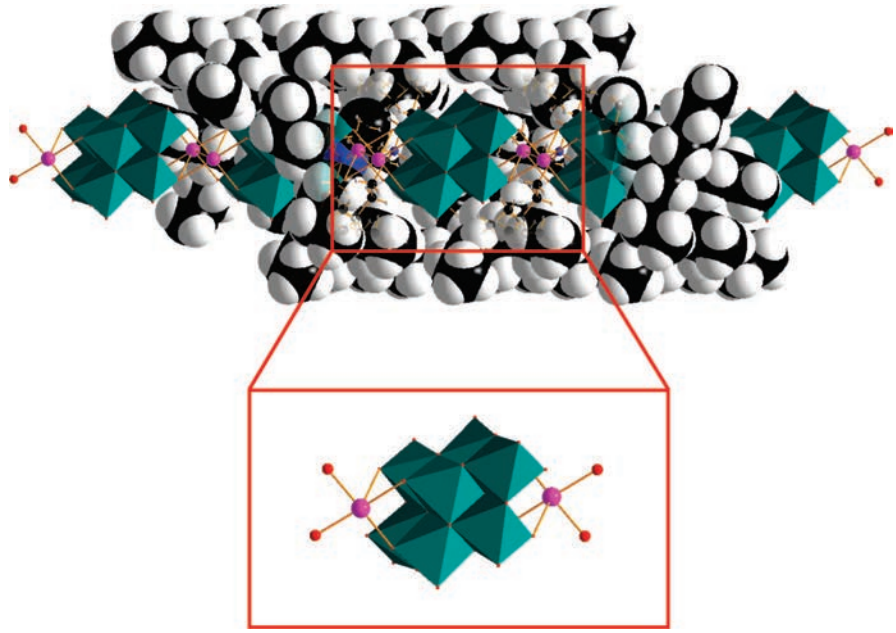

Figure 3. Structural representation of the silver-linked β-octamolybdate chain (ball and stick, and green polyhedra) wrapped in "encapsulating" TBA^+ cations (space-filling representation) which makes up the structure of $TBA_{2n}[Ag_2Mo_8O_{26}]_n$ (**1**). The organic cations are partially removed to reveal the encapsulated chain structure (top). The (Ag{Mo_8}Ag) synthon unit, the building block of this chain, is highlighted below. Color scheme: Mo, green polyhedra; Ag, pink; O, red; N, blue; C, black; H, white.

CSI-MS analyses on the reaction solution of compound **1** and allowed access to directly observe the rearrangement of Lindqvist anions into the (Ag{Mo_8}Ag) synthon units and the subsequent wrapping of the one-dimensional silver-octamolybdate synthons with organic cations. This is a new approach to studying the solution state species involved in the self-assembly of POMs with the general approach adopted to date being dissolution of the prepared crystalline POM into a suitable solvent.[20,21,29,30]

To our knowledge the only experiments carried out using ESI-MS to directly observe a reacting POM solution have been the study of the organosilane functionalization of a Dawson heteropolytungstate cluster,[31] the study of metal interchange between phosphododecatungstates and molybdate anions,[25] and a study of molybdate and tungstate clusters with arylated cations.[32]

Thus far, ESI-MS studies on POM systems have been seen to generate only limited monoanionic series and multiply charged ion fragments.[23,24,33] In contrast, the power of CSI-MS in improving our analytical capabilities in investigating very large, labile POM frameworks is evident immediately on inspection of the following results. Only monoanionic and dianionic series are observed in these results, from approximately 285 *m*/*z* to as high as approximately 3800 *m*/*z*, indicating the efficient transfer of very high nuclearity, yet labile, ionic species into the detector with minimal interfering effects from the ionization and desolvation processes.

The six monoanionic series identified within these results are as follows:

(i) $[Mo_mO_{3m}]^-$ where $m = 2$, 3 or 5
(ii) $[HMo_mO_{3m+1}]^-$ where $m = 2$ to 6
(iii) $[H_7Mo_mO_{3m+2}]^-$ where $m = 2$ to 6
(iv) $[H_7Mo_mO_{3m+3}]^-$ where $m = 2$ to 5
(v) $[H_9Mo_mO_{3m+4}]^-$ where $m = 2$ to 6
(vi) $[AgMo_mO_{3m+1}]^-$ where $m = 2$ to 4

From these identified anion series (see Figure 4) only series (ii) has been observed in previous ESI-MS studies on polyoxomolybdate systems[23] which underpins the advance in understanding that can be made with CSI-MS studies for detecting molecular building blocks.

The silver-containing anion series (vi) is of special interest with regards to this POM reaction system. This is because the role of the Ag^I moiety in the assembly of the stable silver-linked octamolybdate species has been observed by mass spectral methods for the first time and is shown to be crucial for the formation of the larger cluster fragments. This is a highly important result with many possibilities for utilizing new approaches to the self-assembly of large POMs. The detection of fragments of the (Ag{Mo_8}Ag) synthon units, especially $[AgMo_2O_7]^-$ (peak at 410.7 *m*/*z*) and $[AgMo_4O_{13}]^-$ (peak at 700.5 *m*/*z*), are particularly important to understanding the formation of compound **1** from this reaction system (see Figure 4). Detection of the $[AgMo_2O_7]^-$ fragment of the (Ag{Mo_8}Ag) synthon from the reaction solution supports the theory of rearrangement of the Lindqvist anion into $[AgMo_2O_7]^-_n$ which is the smallest stable unit of the silver-linked POM chain. Indeed the stable nature of this fragment of the (Ag{Mo_8}Ag) synthon unit allowed the isolation in the solid state of $Ag_2Mo_2O_7$ clusters by Gatehouse and Leverett in 1976.[34] Detection of the $[AgMo_4O_{13}]^-$ species (peak at 700.5 *m*/*z*), being half-the

(29) Walanda, D. K.; Burns, R. C.; Lawrance, G. A.; von Nagy-Felsobuki, E. I. *Inorg. Chem. Commun.* **1999**, *2*, 487–489.
(30) Walanda, D. K.; Burns, R. C.; Lawrance, G. A.; von Nagy-Felsobuki, E. I. *Inorg. Chim. Acta* **2000**, *305*, 118–126.
(31) Mayer, C. R.; Roch-Marchal, C.; Lavanant, H.; Thouvenot, R.; Sellier, N.; Blais, J. C.; Secheresse, F. *Chem.—Eur. J.* **2004**, *10*, 5517–5523.
(32) Alyea, E. C.; Craig, D.; Dance, I.; Fisher, K.; Willett, G.; Scudder, M. *CrystEngComm* **2005**, *7*, 491–503.
(33) Boglio, C.; Lenoble, G.; Duhayon, C.; Hasenknopf, B.; Thouvenot, R.; Zhang, C.; Howell, R. C.; Burton-Pye, B. P.; Francesconi, L. C.; Lacote, E.; Thorimbert, S.; Malacria, M.; Afonso, C.; Tabet, J. C. *Inorg. Chem.* **2006**, *45*, 1389–1398.

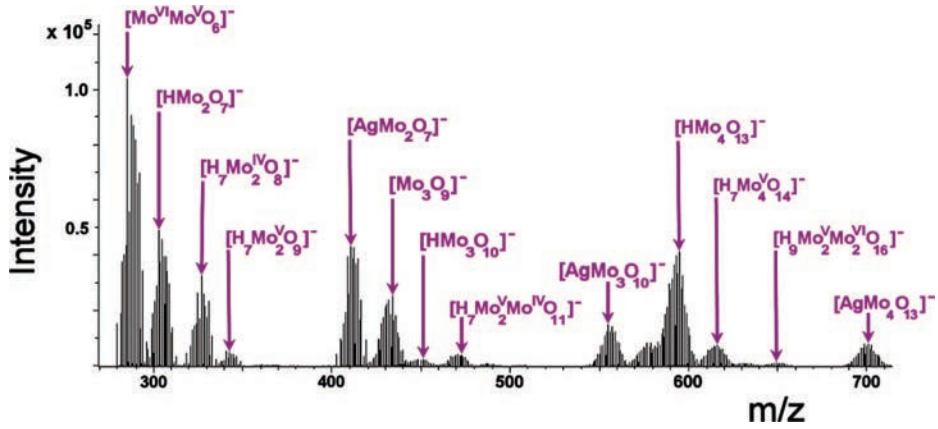

Figure 4. CSI-MS data collected of the reaction solution of **1**. The six monoanionic series identified within these results are highlighted. The steps toward the assembly of the (Ag{Mo_8}Ag) synthon units can be observed by examination of anion series (vi) which highlights the role of Ag^+ in the rearrangement process of these clusters. Of particular note from this series are the peaks at 410.7 *m*/*z* and 700.5 *m*/*z* which are attributed to the species $[AgMo_2O_7]^-$ and $[AgMo_4O_{13}]^-$, respectively.

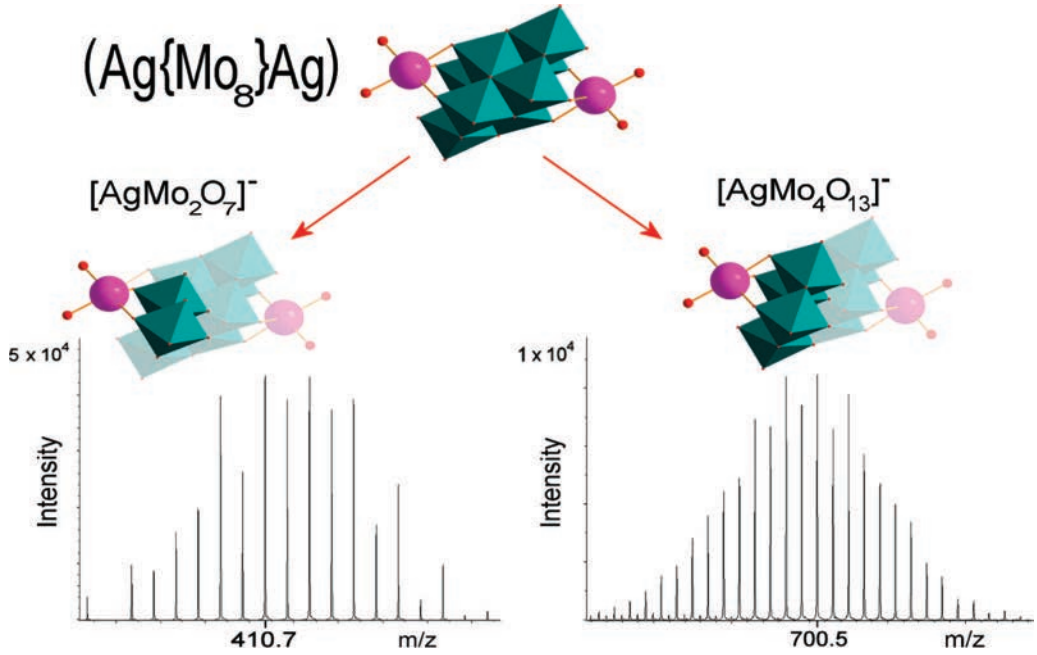

Figure 5. Representation of the $[AgMo_2O_7]^-$ and $[AgMo_4O_{13}]^-$ species identified within the CSI-MS analyses of a reaction solution of **1**. Top: Representation of the $[AgMo_2O_7]^-$ and $[AgMo_4O_{13}]^-$ species as building blocks of the (Ag{Mo_8}Ag) synthon. Bottom: Mass spectra of the isotopic envelopes for their corresponding mass peaks at 410.7 *m*/*z* and 700.5 *m*/*z*, respectively. Color scheme: Mo, green polyhedra; Ag, pink; O, red.

(Ag{Mo_8}Ag) synthon unit, represents the next stepping stone in the final rearrangement to the stable silver-linked octamolybdate species. See Figure 5.

In the higher mass range of the CSI-MS analyses carried out, the structure directing effect of the organic cations, hypothesized by us in previous work, is illustrated for the first time. Detection of the following species $[(AgMo_8O_{26})TBA_2]^-$ (peak at 1776.6 *m*/*z*), $[(Ag_2Mo_8O_{26})(Mo_4O_{13})TBA_3]^-$ (peak at 2718.3 *m*/*z*), and $[(Ag_2Mo_8O_{26})(Mo_8O_{26})TBA_5]^-$ (peak at 3796.5 *m*/*z*), each with an increasing organic cation contribution, shows the increasing metal nuclearity of the chain of compound **1** concomitant with the associated increase in organic cations present (see Figures 6−8). This observation can be interpreted as the start of the self-assembly aggregation process where "monomeric" units assemble into larger fragments which eventually leads to the formation of crystals of compound **1** (see Figure 8). Also this analysis supports the previously proposed hypothesis[17] that the organic cations used in the synthesis do indeed play an important structural role in promoting the mode of POM structure growth in solution.

Another significant observation from these CSI-MS results is the identification of mixed oxidation state species in POM fragments from dimolybdate up to hexamolybdate fragments, where molybdenum is found to exist in oxidation states +4, +5, and +6. This is an important set of observations as although the single reduced molybdate species $[Mo^VO_3]^-$ and the corresponding single reduced tungstate species $[W^VO_6]^-$ have

(34) Gatehouse, B. M.; Leverett, P. *J. Chem. Soc., Dalton Trans.* **1976**, 1316–1320.
(35) Only the peaks that could be unambiguously fitted using simulated spectra were assigned. We are presently developing a fitting approach to more fully assign all the species.

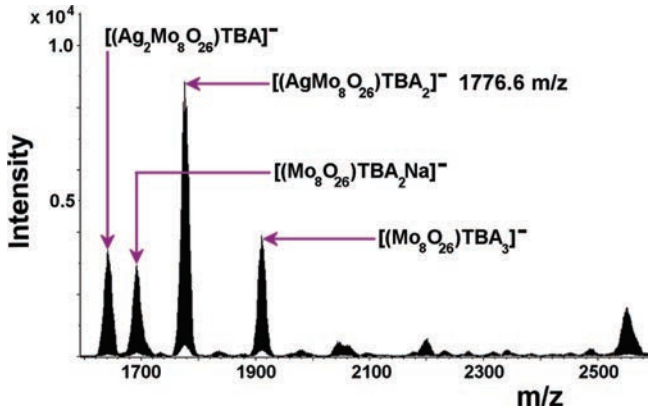

Figure 6. CSI-MS data collected of the reaction solution of **1** over the 1500−2600 *m*/*z* range. Note only the peaks that could be fully assigned are labeled.[35]

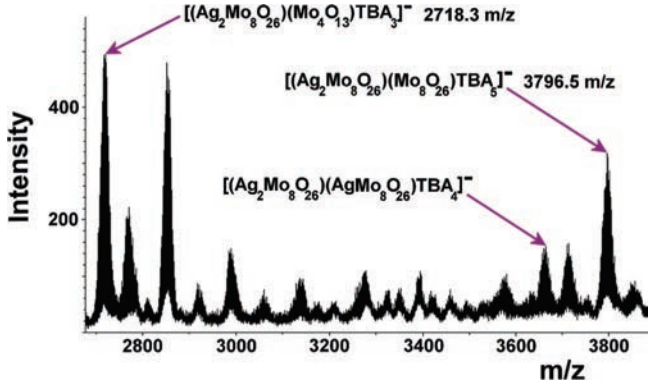

Figure 7. CSI-MS data collected of the reaction solution of **1** over the 2500−6000 *m*/*z* range. Note only the peaks that could be fully assigned a labeled.[35]

Table 1. Hexamolybdate Reagents with Different Chain Length Alkylammonium Cations Used in Reaction Mixtures with AgF, Each Stirred for Only 5 Min Prior to Reaction Monitoring

Reaction Mix **A**	$((n\text{-}C_4H_9)_4N)_2[Mo_6O_{19}]$
Reaction Mix **B**	$((n\text{-}C_5H_{11})_4N)_2[Mo_6O_{19}]$
Reaction Mix **C**	$((n\text{-}C_6H_{13})_4N)_2[Mo_6O_{19}]$
Reaction Mix **D**	$((n\text{-}C_7H_{15})_4N)_2[Mo_6O_{19}]$

been observed previously,[23,24] mixed oxidation state fragments, such as the dimolybdate fragment $[Mo^{VI}Mo^{V}O_6]^-$ (see Figure 9), have, to our knowledge, been observed for the first time.[36] Mixed oxidation state fragments of polyoxochromate systems have, however, been observed previously using ESI-MS. [37]

The CSI-MS analyses described thus far were carried out on the reaction mixture of $TBA_2[Mo_6O_{19}]$ and silver(I) fluoride after stirring overnight, i.e., following the same experimental steps from the reported synthesis of **1**. However, these results then led to further investigations into how rapidly the interconversion from the Lindqvist anion into (Ag{Mo_8}Ag) synthons actually takes place, and whether the length of organic countercation used in the reaction system affects the rate of this rearrangement.

To investigate the kinetics of the rearrangement process of Lindqvist anions into (Ag{Mo_8}Ag) synthons, electronic absorbance studies were used to monitor the decrease of the Lindqvist anion absorption band at $\lambda = 355$ nm over time[38] in a reaction mixture of **1** stirred for only 5 min prior to reaction monitoring (see Reaction Mix **A** in Table 1).

To further support this relationship between decreasing Lindqvist anion concentration as monitored *via* electronic absorbance spectroscopy and concomitant increase in {Mo_8} anion concentration, Reaction Mix **A** was also monitored over time using CSI-MS experiments. During these experiments the CSI-MS method parameters were kept constant throughout. Therefore, although the lack of a suitable internal standard precludes the quantitative analysis of the results, a qualitative relationship between the observed species can be elucidated by monitoring peak intensities over time during the reaction. From these results clear, general trends can be identified in the recorded peak intensities as monitored over the time of reaction for the species $[TBA(Mo_6O_{19})]^-$ (peak at 1122.6 *m*/*z*), $[(AgMo_8O_{26})TBA_2]^-$ (peak at 1776.6 *m*/*z*), and $[(Ag_2Mo_8O_{26})TBA]^-$ (peak at 1643.2 *m*/*z*); see Figure 10. It can be seen from these general trends that the peak intensity of the reagent $[TBA(Mo_6O_{19})]^-$ decreases as the peak intensities recorded for the product species $[(AgMo_8O_{26})TBA_2]^-$ and $[(Ag_2Mo_8O_{26})TBA]^-$ increase. Interestingly, it can also be observed from these CSI-MS results that the recorded peak intensity of species $[AgMo_4O_{13}]^-$ (peak at 700.5 *m*/*z*) over reaction time appears to remain almost constant throughout. This may indicate an equilibrium state of $[AgMo_4O_{13}]^-$ concentration where the rearrangement of Lindqvist anions forms $[AgMo_4O_{13}]^-$ species, which then continue rearranging into the larger reactive (Ag{Mo_8}Ag) building blocks.

The effect of the length of organic countercation used in the reaction system on the rate of Lindqvist to (Ag{Mo_8}Ag) synthon rearrangement was then investigated using electronic absorbance spectroscopy studies on Reaction Mix **A**−**D**; see Table 1. These studies were carried out in the same way as described previously for Reaction Mix **A**. Comparison of the pseudo first-order rate constants, with respect to [{Mo_6}], calculated over the first 75 min of each reaction reveals the general trend that the rate of decrease in the concentration of Lindqvist anions, and as a result the interconversion of Lindqvist into β-octamolybdate anions, decreases as the carbon chain length of the alkylammonium cations increases; see Figure 11 and Table SI6 in the Supporting Information.[39]

There is a slight discrepancy in this general trend with the observed rate constant for the tetrapentylammonium cation calculated at approximately 0.6×10^{-4} s^{-1} higher than that for the tetrabutylammonium cation. This may be due to the tetrapentyl side chains representing the maximum cation steric bulk which can be accommodated by the {Mo_6} to {Mo_8} interconversion before the reaction rate is slowed significantly, as per the tetrahexyl and tetraheptyl side chains.

(36) It should be noted that that the observation of the reduced POM units at low mass could be a result of the voltage effects (e.g., ion transfer voltages and high collision energy voltage at low mass) utilized in the technique of mass spectrometry to investigate fragment ion species at low mass.

(37) Sahureka, F.; Burns, R. C.; von Nagy-Felsobuki, E. I. *Inorg. Chim. Acta* **2002**, *332*, 7–17.

(38) Li, Q.; Wu, P. F.; Xia, Y.; Wei, Y. G.; Guo, H. Y. *J. Organomet. Chem.* **2006**, *691*, 1223–1228.

(39) Comparison of the pseudo-first-order rate constants reveals the general trend that the rate of decrease in the concentration of Lindqvist anions decreases as the carbon chain length of the alkylammonium cations increases. However, it should be noted that the absolute figures of these rate constants will vary according to changes in experimental parameters such as temperature variation, filtration time prior to kinetic monitoring, and the human error introduced by the time needed in the solution preparation process.

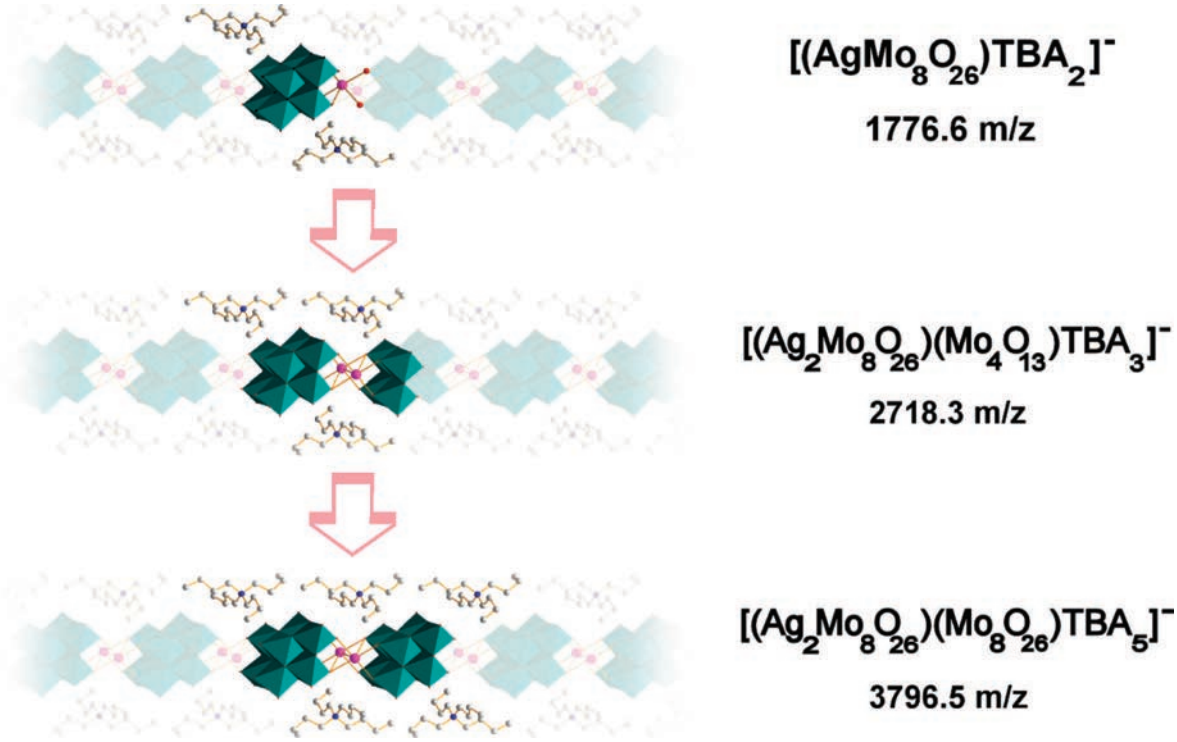

Figure 8. Structural representation of the higher mass fragments (highlighted) identified within the CSI-MS analyses of a reaction solution of **1**. This diagram illustrates the increasing metal nuclearity of the chain of compound **1** concomitant with the associated increase in organic cations present. Color scheme: Mo, green polyhedra; Ag, pink; O, red; C, gray; N, blue.

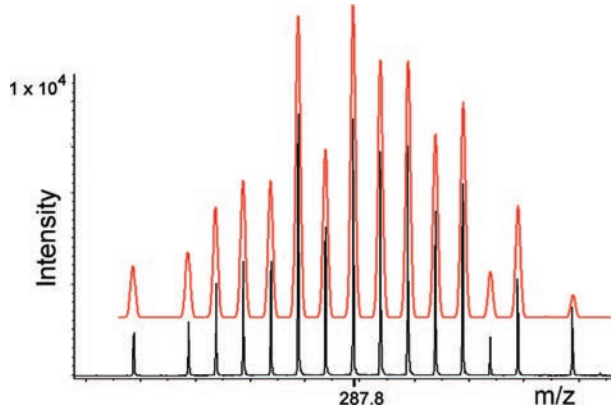

Figure 9. Comparison of the experimental (black spectrum) and simulated (superimposed red spectrum) isotopic envelope for the peak at 287.8 *m*/*z* recorded during CSI-MS analyses of a reaction solution of **1**. Through this comparison this peak can be clearly identified as the mixed oxidation state dimolybdate species $[Mo^{VI}Mo^{V}O_6]^-$. Unambiguous identification of small species such as this is accessible in this manner only when the isotopic patterns for the species are very distinct, as for the spectrum shown above.

A possible explanation for the lower rates of interconversion of Lindqvist anions into the β-octamolybdate anions observed in Reaction Mix **C** and **D** may be attributed to the long chain, large steric bulk cations hindering the rearrangement of Lindqvist anions by both being too sterically hindering to promote formation of the (Ag{Mo_8}Ag) synthons *via* wrapping around them as effectively as the smaller chain tetrabutylammonium cations, and also by hindering contact between the silver cations and molybdenum anions. These results also appear to support the previously proposed hypothesis that the steric bulk of the alkylammonium cations present in a reaction system influences the (Ag{Mo_8}Ag) synthon-containing crystal structures which can be isolated in the solid state from these reaction mixtures.[17,32]

Conclusions

In conclusion CSI-MS has been used to elucidate the solution state rearrangement of POM clusters for the first time. Specifically the role of the Ag^I ions in the assembly of the stable, silver-linked β-octamolybdate structure **1** has been revealed using mass spectral investigations. The identification of anion series (vi), i.e., $[AgMo_mO_{3m+1}]^-$ where $m = 2$ to 4, in particular the $[AgMo_2O_7]^-$ and $[AgMo_4O_{13}]^-$ fragments of the (Ag{Mo_8}Ag) synthon units, are of significance in understanding the formation of compound **1** from this reaction system. Also monoanionic series involving mixed oxidation state polyoxomolybdate species, from dimolybdate up to hexamolybdate fragments, have been observed for the first time.[36] Detection, in the CSI-MS analyses, of the species $[(AgMo_8O_{26})TBA_2]^-$, $[(Ag_2Mo_8O_{26})(Mo_4O_{13})TBA_3]^-$, and $[(Ag_2Mo_8O_{26})(Mo_8O_{26})TBA_5]^-$, each with an increasing organic cation contribution, supports the previously proposed hypothesis[17] that the organic cations used in the synthesis do indeed play an important structure-directing role in promoting the mode of POM structure growth in solution.

The rate of decrease in Lindqvist anion concentration and, therefore, concomitant increase in {Mo_8} anion concentration, for Reaction Mixtures **A**−**D**, were monitored *via* electronic absorbance spectroscopy. This correlation between decreasing Lindqvist anion and increasing {Mo_8} anion concentration was supported by CSI-MS monitoring of Reaction Mix **A**, i.e., $TBA_2[Mo_6O_{19}]$ + AgF, over time. The use of CSI-MS in this way to monitor real-time, in-solution rearrangements in a POM reactant solution is, to our knowledge, unprecedented. This approach can now be extended to investigate the bottom-up, in-solution processes governing the formation of other POM

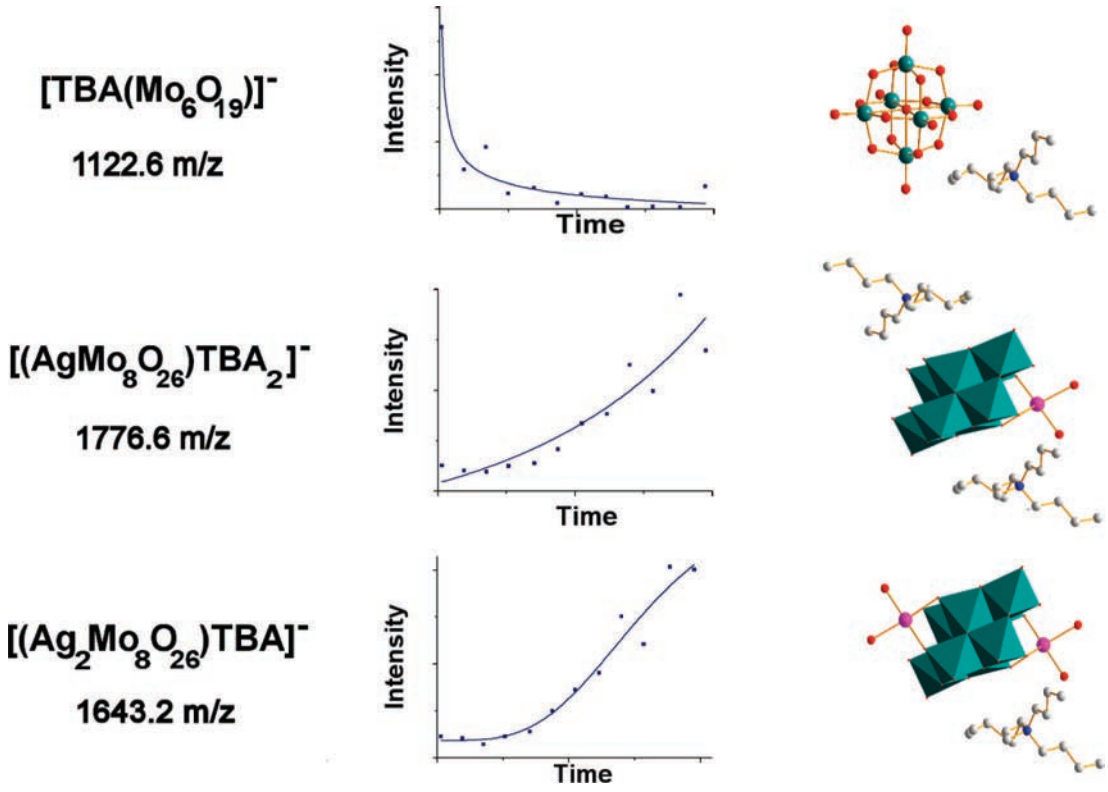

Figure 10. Graphs showing peak intensities plotted against the time of CSI-MS data acquisition during the reaction of $TBA_2[Mo_6O_{19}]$ + AgF, i.e., Reaction Mix **A** (best fits shown). The peak identities and *m*/*z* values of the peaks studied are shown (left) along with representations of the predicted structures of these species (right). Top: $[TBA(Mo_6O_{19})]^-$ at 1122.6 *m*/*z*. Center: $[(AgMo_8O_{26})TBA_2]^-$ at 1776.6 *m*/*z*. Bottom: $[(Ag_2Mo_8O_{26})TBA]^-$ at 1643.2 *m*/*z*. Color scheme: Mo, green polyhedra; Ag, pink; O, red; C, gray; N, blue.

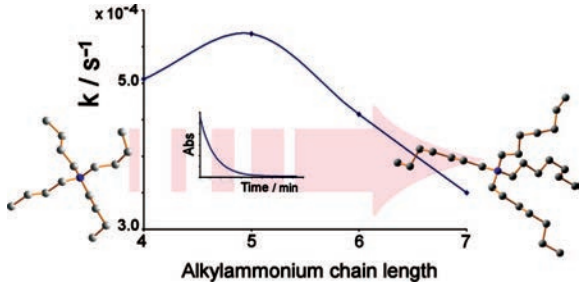

Figure 11. Graph showing the pseudo-first-order rate constants, calculated using data from electronic absorbance spectroscopy studies of Reaction Mix **A**−**D**, plotted against the carbon chain length of the alkylammonium cation used.[39] The blue line is used as a guide for the eye. Inset: Decrease of the Lindqvist anion absorption band at $\lambda = 355$ nm over time in Reaction Mix **D**. Also shown are ball and stick representations of the tetrabutylammonium cation and the much more sterically hindering tetraheptylammonium cation. Color scheme: C, gray; N, blue.

systems so enhancing our understanding and giving us the potential to control the building-block principles involved.

The effect of the length of the organic countercation used in the reaction system on the rate of Lindqvist to (Ag{Mo_8}Ag) synthon rearrangement was examined *via* comparison of the pseudo-first-order rate constants, with respect to [{Mo_6}], calculated over the first 75 min in the electronic absorbance experiment for each reaction mix. The general trend observed from these calculated rate constants was that the rate of decrease in the concentration of Lindqvist anions, and as a result the interconversion of Lindqvist into β-octamolybdate anions, decreases as the carbon chain length of the alkylammonium cations increases.[39] These lower rates of interconversion when using a hexamolybdate reagent with a longer chain cation may be attributed to the steric bulk of these large organic groups hindering the rearrangement of Lindqvist anions and hindering contact between the silver cations and molybdenum anions. These results, therefore, support the previously proposed hypothesis that the steric bulk of the alkylammonium cations present in a reaction system influences the (Ag{Mo_8}Ag) synthon-containing POM structures which can be formed and then isolated in the solid state from these reaction mixtures.[17,32]

Future work will involve applying a similar integrated analysis approach to analyzing the self-assembly processes governing the formation of POM structures in different reaction systems. Utilizing the power of CSI-MS to investigate very large, labile POM frameworks in conjunction with the use of other analytical techniques such as electronic absorbance spectroscopy will allow further exploration and expansion of our understanding of the building block principles which govern these bottom-up processes in solution and will lead us to future methods for control of these building processes. We will also investigate a CSI-MS quantitative analysis of the species involved in the assembly process after the development of suitable internal standards.

Experimental Section

Sample Preparation. Reaction Mixture (**1**) for CSI-MS analysis: Silver(I) fluoride (28 mg, 0.22 mmol) suspended in methanol (3 mL) by sonication was added to a solution of $TBA_2[Mo_6O_{19}]$ (150 mg, 0.11 mmol) in acetonitrile (4 mL). When left to stir overnight at room temperature, a cloudy white solution was formed. Filtration of this solution produced a clear colorless solution. (This is the first stage of the synthesis of $TBA_{2n}[Ag_2Mo_8O_{26}]_n$ (**1**).) From this solution 20 μL were removed and made up to 2 mL with acetonitrile to produce a 1×10^{-4} mol L^{-1} dilution suitable for MS testing.

Reaction Mixture **A** for CSI-MS, time monitored experiments: Silver(I) fluoride (28 mg, 0.22 mmol) suspended in methanol (3 mL) by sonication, was added to a solution of $TBA_2[Mo_6O_{19}]$ (150 mg, 0.11 mmol) in acetonitrile (4 mL). This solution was stirred, protected from light, for 5 min at room temperature then filtered. The solution was then kept in the dark throughout the experiment. The reaction was timed from when the first 20 μL aliquot of this solution was made up to 2 mL with acetonitrile to produce the first 1×10^{-4} mol L^{-1} dilution suitable for MS testing. The time of removal of each 20 μL aliquot to make up MS dilutions was noted throughout this experiment, with the final dilution made up ~195 min after the first dilution.

Reaction Mixture **A** for electronic absorbance, time monitored experiments: Silver(I) fluoride (28 mg, 0.22 mmol) suspended in methanol (3 mL) by sonication was added to a solution of $TBA_2[Mo_6O_{19}]$ (150 mg, 0.11 mmol) in acetonitrile (4 mL). This solution was stirred, protected from light, for 5 min at room temperature and then filtered. From this solution 126 μL were removed and made up to 4 mL with acetonitrile/methanol (40:30) solvent to produce a 5×10^{-4} mol L^{-1} dilution suitable for electronic absorbance testing.

This preparation method is repeated replacing $((n\text{-}C_4H_9)_4N)_2[Mo_6O_{19}]$ with $((n\text{-}C_5H_{11})_4N)_2[Mo_6O_{19}]$ (162 mg, 0.11 mmol), $((n\text{-}C_6H_{13})_4N)_2[Mo_6O_{19}]$ (175 mg, 0.11 mmol), or $((n\text{-}C_7H_{15})_4N)_2[Mo_6O_{19}]$ (187 mg, 0.11 mmol), to produce Reaction Mix **B**, **C**, or **D** respectively for electronic absorbance, time monitored experiments.

To calculate the molar absorption coefficient values for each tetraalkylammonium hexamolybdate compound used in the electronic absorbance experiments, the method described above was repeated for each alkylammonium hexamolybdate solution, except in the absence of silver(I) fluoride.

CSI-MS Experimental and Analyses. All MS data were collected using a Q-trap, time-of-flight MS (MicrOTOF-Q MS) instrument supplied by Bruker Daltonics Ltd. A cryospray source, also supplied by Bruker Ltd., was used to collect data under the conditions specified below. The detector was a time-of-flight, microchannel plate detector, and all data were processed using the Bruker Daltonics Data Analysis 3.4 software, while simulated isotope patterns were investigated using Bruker Isotope Pattern software and Molecular Weight Calculator 6.45.

The following parameters were consistent for all CSI-MS scans given below. The calibration solution used was Agilent ES tuning mix solution, Recorder No. G2421A, enabling calibration between ~100 *m*/*z* and 3000 *m*/*z*. This solution was diluted 60:1 with acetonitrile. Samples were introduced into the MS *via* direct injection at 180 μL/h. The cryospray settings were set with the sprayer nitrogen gas temperature at −40 °C and the drying nitrogen gas temperature at −20 °C. The ion polarity for all MS scans recorded was negative, with the voltage of the capillary tip set at 4000 V, end plate offset at −500 V, funnel 1RF at 300 Vpp, and funnel 2 RF at 400 Vpp. Other MS parameters, which are set to specific values for each scan, are given below in tabular format.

	scan of mass range		
MS parameter	50−1500 *m*/*z*	1500−2600 *m*/*z*	2500−6000 *m*/*z*
hexapole RF/Vpp	400	700	700
ion energy/eV/z	−5	−5	−5
low mass/*m*/*z*	600	400	400
collision energy/eV/z	−100	−20	−30
collision cell RF/Vpp	500	1200	1500
transfer time/μs	120	150	150
prepulse storage time/μs	5	40	40
summation	5000	30000	30000
time of acquisition/min	1	3	3
active focus	ON	OFF	OFF

All theoretical peak assignments were determined via comparison of the experimentally determined isotopic patterns for each peak, with simulated isotopic patterns. For relatively small POM fragments, e.g., up to approximately $[Mo_6O_{19}]^{2-}$, the isotopic pattern is quite distinct and comparison between experimental and simulated patterns is more meaningful (see Figure 9) than in the case of larger fragments where the isotopic pattern takes on a Gaussian shape and it cannot be said with certainty that the suggested peak is unequivocally correct.

CSI-MS, Time Monitored Experiments. For all data acquisitions in these experiments the CSI-MS method parameters used were as those given in the parameter table above for the mass ranges 50−1500 *m*/*z* and 1500−2600 *m*/*z*. These parameters were consistent for all CSI-MS scans.

Electronic Absorbance Spectroscopy. All electronic absorbance data were collected using a UV-1700 PharmaSpec spectrophotometer supplied by Shimadzu. The spectral data collected to determine the molar absorption coefficient values for each alkylammonium hexamolybdate used in this study were recorded over the wavelength range 500 to 190 nm, using the same concentration hexamolybdate solutions as used when investigating the Reaction Mixtures **A**−**D**. The kinetic data collected involved the recording of the absorbance count at 355 nm (λ chosen to avoid overlap of different species) at 20 s intervals over a period of 75 min after the UV dilution of each reaction mixture was placed in the instrument.

Acknowledgment. This work was supported by the EPSRC, University of Glasgow, and WestCHEM. We thank Bruker Daltonics Ltd. for collaboration and support.

Supporting Information Available: Crystallographic data; sample preparation details; CSI-MS experimental, analyses, and spectra; electronic absorbance spectroscopy experimental and data. This information is available free of charge via the Internet at http://pubs.acs.org/.

JA802514Q